

A Quantitative Method to Determine What Collisions Are Reasonably Foreseeable and Preventable

Erwin de Gelder^{a,*}, Olaf Op den Camp^a

^a*TNO, Integrated Vehicle Safety, Helmond, The Netherlands*

Abstract

The development of Automated Driving Systems (ADSs) has made significant progress in the last years. To enable the deployment of Automated Vehicles (AVs) equipped with such ADSs, regulations concerning the approval of these systems need to be established. In 2021, the World Forum for Harmonization of Vehicle Regulations has approved a new United Nations regulation concerning the approval of Automated Lane Keeping Systems (ALKSs). An important aspect of this regulation is that “the activated system shall not cause any collisions that are reasonably foreseeable and preventable.” The phrasing of “reasonably foreseeable and preventable” might be subjected to different interpretations and, therefore, this might result in disagreements among AV developers and the authorities that are requested to approve AVs.

The objective of this work is to propose a method for quantifying what is “reasonably foreseeable and preventable”. The proposed method considers the Operational Design Domain (ODD) of the system and can be applied to any ODD. Having a quantitative method for determining what is reasonably foreseeable and preventable provides developers, authorities, and the users of ADSs a better understanding of the residual risks to be expected when deploying these systems in real traffic.

Using our proposed method, we can estimate what collisions are reasonably foreseeable and preventable. This will help in setting requirements regarding the safety of ADSs and can lead to stronger justification for design decisions and test coverage for developing ADSs.

Keywords: Safety; Automated Driving System; Automated Vehicle; Automated Lane Keeping System; Reasonably foreseeable; Preventable

1. Introduction

It is generally expected that Automated Driving Systems (ADSs) will make traffic safer by eliminating human errors, enable more comfortable rides, and reduce traffic congestion (Chan, 2017). Lower levels of automation systems, such as adaptive cruise control (Mahdinia et al., 2020) and lane keeping assist systems

*Corresponding author

(Mammeri et al., 2015), are already widely deployed in modern cars and trucks. Since the development of ADSs has made significant progress, it is expected that ADSs addressing higher levels of automation and covering the full dynamic driving task, i.e., SAE level 3 or higher (SAE J3016, 2021), are soon to be introduced on public roads (Bimbraw, 2015; Milakis et al., 2016; Madni, 2018).

The main idea of an ADS is to either assist the driver with its driving task or to take over certain driving tasks. For higher levels of automation, the ADS may (temporarily) take over the full driving task of the driver. A potential hindrance to the deployment of higher levels of automation is the Vienna Convention on road traffic of 1968. This convention, which is the basis of the national traffic laws of a large number of countries, requires that a human driver is in charge of driving (Vellinga, 2019). Given the time at which the Vienna Convention has been drafted, it is not unreasonable that it has been assumed that a human is always in charge of the driving task. Clearly, new regulations concerning the approval of higher levels of automation are needed.

To address the lack of a notion of an automated system that takes over the driving task of a human driver in the Vienna Convention, in 2021, the World Forum for Harmonization of Vehicle Regulations has approved a new United Nations regulation concerning the approval of an ADS, with the title “uniform provisions concerning the approval of vehicles with regard to automated lane keeping systems” (E/ECE/TRANS/505/Rev.3/Add.156, 2021). Regarding the system safety and fail-safe response, the following requirement is mentioned (E/ECE/TRANS/505/Rev.3/Add.156, 2021, Chapter 5): “The activated system shall not cause any collisions that are reasonably foreseeable and preventable.” This requirement leaves room for different interpretations, because the terms “reasonably foreseeable” and “preventable” have not been quantified. The different interpretations might result in disagreements among ADS developers and the authorities that are requested to approve an ADS.

To provide more clarity on the terms “reasonably foreseeable” and “preventable”, several studies are published. Schoener (2020) provides examples of scenarios that are (not) foreseeable and in which collisions are (not) preventable. This gives some directions, although the terms are not further quantified. In the regulation itself, it is mentioned that “the threshold for preventable/unpreventable is based on the simulated performance of a skilled and attentive human driver” (E/ECE/TRANS/505/Rev.3/Add.156, 2021, Chapter 3). This is further exploited by Mattas et al. (2022), where four different driver behavior models are considered in parameterized scenarios and in each scenario, it is checked whether the driver could avoid a collision. Two of these four driver behavior models are also presented in an amendment of the aforementioned regulation, see (ECE/TRANS/WP.29/2022/59/Rev.1, 2022, Annex 3, Clauses 3.3 and 3.4). In (Kusano et al., 2022), the collision avoidance performance of the Waymo ADS is compared with that of a Non-Impaired Eyes ON the conflict (NIEON) reference behavior model. Nakamura et al. (2022); Muslim et al. (2023) provide a method to determine the range of the parameter values of “foreseeable” scenarios. This is done by fitting parametric distributions to the scenario parameter values and determining a

range of the values that capture, e.g., 99 %, of the probability mass. In (Kusano et al., 2022), based on the analysis of driving data from instrumented Waymo vehicles and a set of so-called core scenarios identified earlier, new scenarios are created. These new scenarios may not have been observed in the driving data, but are still deemed to be reasonably foreseeable such that they are considered during the safety evaluation.

We assume that “reasonably foreseeable” refers to the scenarios that are potentially leading to a collision. If a scenario is reasonably foreseeable, it is expected from the developers to consider this scenario during the design process and, therefore, ensure that the ADS safely handles such a scenario so that no collision occurs in this scenario. Hence, this work addresses the following research question:

Research question 1. *How to determine what are reasonably foreseeable scenarios?*

To answer this research question, we follow a similar approach as (Nakamura et al., 2022; Muslim et al., 2023), i.e., based on scenarios extracted from real-world data, we estimate the range of the scenario parameters that are reasonably foreseeable. To estimate this range, a Probability Density Function (PDF) of the scenario parameters is estimated. This range of parameters is such that the probability of encountering a scenario with parameter values outside this range is below a threshold. Two different approaches are used for estimating the PDF of the scenario parameters. The first approach employs the non-parametric PDF estimation technique called Kernel Density Estimation (KDE). Therefore, in contrast to the work of Nakamura et al. (2022); Muslim et al. (2023), no assumptions are needed regarding a parametric distribution and the independence of the scenario parameters. The second approach uses only part of the data that is above a certain threshold, such that the Generalized Pareto Distribution (GPD) can be assumed according to the Extreme Value Theory (EVT). Both approaches come with advantages and disadvantages which will be discussed in this work.

The other term in the aforementioned requirement of the regulation (E/ECE/TRANS/505/Rev.3/Add.156, 2021) that leaves room for different interpretations is “reasonably preventable”. To make this more measurable, this work also proposes a method to answer the following question:

Research question 2. *How to determine to which extent collisions are reasonably preventable?*

We propose two alternative approaches that follow the Automated Lane Keeping System (ALKS) regulation that mentions that “the threshold for preventable/unpreventable is based on the simulated performance of a skilled and attentive human driver” (E/ECE/TRANS/505/Rev.3/Add.156, 2021, Chapter 3). The first approach is to study to which extent a skilled and attentive human avoids a collision considering a certain *type of scenario*. This is estimated using Monte Carlo simulations while sampling the scenario parameters from the PDF estimated using KDE. Importance sampling is used to reduce the number of required simulations. The second approach is to study to which extent a skilled and attentive human avoids a collision considering a certain *scenario with specific parameter values*. This approach leads to a range of parameter values for which the probability that a skilled and attentive human avoids a collision is above a certain threshold. Of

Table 1: Terms and definitions that are used in this work.

Term	Definition
ODD	Operating conditions under which a given driving automation system or feature thereof is specifically designed to function, including, but not limited to, environmental, geographical, and time-of-day restrictions, and/or the requisite presence or absence of certain traffic or roadway characteristics (SAE J3016, 2021)
Scenario	Quantitative description of the relevant characteristics and activities and/or goals of the ego vehicle(s), the static environment, the dynamic environment, and all events that are relevant to the ego vehicle(s) within the time interval between the first and the last relevant event (de Gelder et al., 2022)
Scenario category	Qualitative description of the relevant characteristics and activities and/or goals of the ego vehicle(s), the static environment, and the dynamic environment (de Gelder et al., 2022)
Reasonably foreseeable	Likelihood of encountering in real-life is above a certain threshold
Preventable	Avoidable by a skilled and attentive human driver

the two proposed approaches, the latter is mostly in line with the method proposed by Mattas et al. (2022) and in the annexes of (ECE/TRANS/WP.29/2022/59/Rev.1, 2022), but our approach differs in that we consider different outcomes when a single scenario is simulated multiple times due to the stochastic nature of the simulations. Whereas in (Mattas et al., 2022), a scenario either results in a collision or not, in our case, each scenario has a probability of a collision between 0 and 1. We also provide a method to assess the certainty of the result, which can be used as a stop criterion for conducting further simulations.

This work is organized as follows. Section 2 proposes the two methods to answer Research questions 1 and 2. To illustrate the proposed methods and as a proof of concept, a case study is presented in Section 3. After the discussion in Section 4, this work is concluded in Section 5.

2. Methodology

Table 1 presents the definitions of the terms that are used in our proposed method. In this work, the probability of u is denoted by $P(u)$, while $E[u]$ denotes the expectation of u . In the following subsection, we propose a method for answering Research question 1. Next, Section 2.2 presents a method for answering Research question 2.

2.1. Determining what reasonably foreseeable means

To answer Research question 1, this section proposes a novel method for quantifying the set of scenarios that are reasonably foreseeable. To quantify “reasonably foreseeable”, we use a threshold denoted by ϵ_F . This threshold ϵ_F has units “per hour”. We propose a method to look for a parameter range such that the likelihood of encountering scenarios with its parameters outside this parameter range equals ϵ_F . This proposed method consists of three steps:

1. Identify the scenarios that are part of the so-called Operational Design Domain (ODD) of the ADS.
2. Determine the exposure of these scenarios, i.e., the expected number of occurrences per hour of driving.
3. Determine the probability of encountering scenarios within a specified parameter range.

The first two steps are explained in Sections 2.1.1 and 2.1.2, respectively. Two different approaches for the third step are presented in Sections 2.1.3 and 2.1.4.

2.1.1. Identification of scenarios

An ADS is designed to operate within its ODD, which is defined by the ADS developer and typically consists of a geofence and some known operational conditions, e.g., see (General Motors, 2018; Aurora, 2019; Waymo, 2021). Once deployed, the ADS needs to deal with many scenarios and the ODD in which the ADS is operating determines the variety of these scenarios. To determine the reasonably foreseeable scenarios, the ODD needs to be known.

Considering the wide variety of scenarios, we propose to distinguish between quantitative scenarios and qualitative scenarios, where scenario categories refer to the latter, see Table 1. It is assumed that all possible scenarios within a given ODD can be categorized into one or more scenario categories. This assumption does not limit the applicability of the methodology proposed in this work, though it might require many scenario categories to describe all these scenarios. In the remainder of this section, we propose a method to determine the set of scenarios within a scenario category \mathcal{C} , where \mathcal{C} denotes a scenario category. For example, a scenario category could refer to all cut-in scenarios in the ODD of the ADS. See (de Gelder et al., 2020b) for more examples of scenario categories.

2.1.2. Probability of exposure

To determine the exposure, we estimate the expected number of encounters of a scenario that belongs to scenario category \mathcal{C} . Let $n_{\mathcal{C}}$ denote the number of encounters per unit of time of a scenario belonging to scenario category \mathcal{C} . We express the exposure as $\mathbb{E}[n_{\mathcal{C}}]$, i.e., the expected number of encounters per unit of time of a scenario belonging to scenario category \mathcal{C} :

$$\mathbb{E}[n_{\mathcal{C}}] = \sum_{n=1}^{\infty} n \mathbb{P}(n_{\mathcal{C}} = n), \quad (1)$$

where $\mathbb{P}(n_{\mathcal{C}} = n)$ denotes the probability of encountering n scenarios belonging to scenario category \mathcal{C} in one hour of driving.

We propose to determine $\mathbb{P}(n_{\mathcal{C}} = n)$, $n = 0, 1, 2, \dots$, based on data, because the data provide a quantitative way to estimate $\mathbb{P}(n_{\mathcal{C}} = n)$. Furthermore, assuming that the data are collected with the same conditions as specified by the ODD of the ADS, the data provides an objective way to estimate $\mathbb{P}(n_{\mathcal{C}} = n)$. The probability can be estimated by counting the number of occurrences of the scenarios in the data. The method to find the scenarios belonging to \mathcal{C} is explained in (de Gelder et al., 2020a): First, tags are used to describe

activities, such as lane changing and braking, and statuses, such as “leading vehicle” and “driving slower”. Note that a tag is typically associated with an object and has a start time and an end time. Second, by searching for a particular combination of these tags that describes the scenario category \mathcal{C} , the start and end time of the scenarios are found.

2.1.3. Estimate parameter range with estimated probability density function

Let $x \in \mathbb{R}^d$ denote the d -dimensional parameter vector that describes a scenario. To estimate the probability that x is within a the range $[x_L, x_U]$, we need to know the Cumulative Distribution Function (CDF) of x . To estimate the CDF, we will first estimate the PDF. Let $f_{\mathcal{C}}(\cdot)$ denote the PDF of the parameters of the scenarios from scenario category \mathcal{C} . Typically, the PDF $f_{\mathcal{C}}(\cdot)$ is unknown, so it needs to be estimated. To estimate the PDF, we use the observed scenarios that have also been used to estimate the exposure (Section 2.1.2). Since the shape of the PDF is also unknown beforehand, assuming a predefined functional form of the PDF for which certain parameters are fitted to the data may lead to inaccurate fits unless a lot of hand-tuning is applied. As an alternative, we propose to estimate $f_{\mathcal{C}}(\cdot)$ using KDE (Rosenblatt, 1956; Parzen, 1962). Let $\{x_i\}_{i=1}^N$ denote the set of parameters of the N observed scenarios that belong to the scenario category \mathcal{C} , then the density $f_{\mathcal{C}}(\cdot)$ is estimated by

$$\hat{f}_{\mathcal{C}}(x) = \frac{1}{Nh^d} \sum_{i=1}^N K\left(\frac{1}{h}(x - x_i)\right). \quad (2)$$

Here, $K(\cdot)$ is the so-called kernel and h is the bandwidth. The choice of the kernel function is not as important as the choice of the bandwidth (Turlach, 1993; Duong, 2007). We use the often-used Gaussian kernel, which is given by

$$K(u) = \frac{1}{(2\pi)^{d/2}} \exp\left\{-\frac{1}{2}\|u\|_2^2\right\}, \quad (3)$$

where $\|u\|_2^2 = u^T u$ denotes the squared 2-norm of u .

The bandwidth $h > 0$ is a free parameter that controls the width of the kernel. A larger bandwidth results in a smoother PDF, but choosing h too large may result in loss of details in the PDF. Methods for estimating the bandwidth range from simple reference rules like Silverman’s rule of thumb (Silverman, 1986) to more elaborate methods (Turlach, 1993). We use leave-one-out cross validation to determine the optimal bandwidth because this minimizes the Kullback-Leibler divergence between the estimated PDF, $\hat{f}_{\mathcal{C}}(\cdot)$, and the unknown PDF that underlies the data, $f_{\mathcal{C}}(\cdot)$ (Turlach, 1993). Because the same amount of smoothing is applied in every direction, the data are first normalized such that the standard deviation equals 1 for each of the d parameters.

Using the estimated PDF of the form of Eq. (2), the estimated CDF is obtained by integrating $\hat{f}_{\mathcal{C}}(x)$. More explicitly, the estimated CDF equals:

$$\hat{F}_{\mathcal{C}}(x) = \int_{-\infty}^{(x)_1} \cdots \int_{-\infty}^{(x)_d} \hat{f}_{\mathcal{C}}(x) \, d(x)_1 \cdots d(x)_d, \quad (4)$$

where $(x)_j$ denotes the j -th entry of the vector x . Using the Gaussian kernel of Eq. (3), this gives

$$\hat{F}_{\mathcal{C}}(x) = \frac{1}{N} \sum_{i=1}^N \prod_{j=1}^d \left[\frac{1}{2} + \frac{1}{2} \operatorname{erf} \left\{ \frac{(x)_j - (x_i)_j}{h\sqrt{2}} \right\} \right], \quad (5)$$

where $\operatorname{erf}\{\cdot\}$ is the error function that is defined as

$$\operatorname{erf}\{u\} = \frac{2}{\sqrt{\pi}} \int_0^u \exp\{-v^2\} dv. \quad (6)$$

The probability $\mathbb{P}(x \in [x_L, x_U])$, i.e., x is within the range $[x_L, x_U]$, is estimated using the evaluation of the estimated CDF, $\hat{F}_{\mathcal{C}}(\cdot)$, at the vertices of the hyperrectangle spanned by x_L and x_U . In case of $d = 1$, this would simply be:

$$\mathbb{P}(x \in [x_L, x_U]) \approx \hat{F}_{\mathcal{C}}(x_U) - \hat{F}_{\mathcal{C}}(x_L). \quad (7)$$

By solving the following equation with respect to x_L and x_U , the range of parameters that are reasonably foreseeable can be determined:

$$\mathbb{E}[n_{\mathcal{C}}] \cdot (1 - \mathbb{P}(x \in [x_L, x_U])) = \epsilon_F. \quad (8)$$

Here, ϵ_F is a threshold with units “per hour”, such that the probability of encountering a scenario of scenario category \mathcal{C} with its parameters outside the range $[x_L, x_U]$ equals ϵ_F . Note that typically multiple solutions for x_L and x_U exist.

2.1.4. Estimate parameter range using extreme values

It might be difficult to justify a particular distribution of the scenario parameters. Therefore, as explained in Section 2.1.3, a non-parametric method for estimating the PDF of the scenario parameters is adopted, such that there is no need to assume a particular shape of the PDF. Nevertheless, our second approach for determining the parameter range makes use of a parametric distribution, namely the Generalized Pareto Distribution (GPD). As we will explain next, according to the Extreme Value Theory (EVT), this choice is justified as long as we only use the data that is above a certain threshold (Franke et al., 2004).

Just as in Section 2.1.3, let us assume that we have a set of parameter values, denoted by $\{x_i\}_{i=1}^N$, with $x_i \in \mathbb{R}^d$. For now, let us assume that $d = 1$. We will discuss the generalization toward multiple parameters at the end of this section. Let u denote the threshold such that we only consider the parameters that are larger than u . To describe this mathematically, let

$$L(u) = \{i; x_i > u\} \quad (9)$$

denote the set of indices for which the parameter values are larger than u . Based on this, we can define a set of “excess values”:

$$\{y_l\}_{l=1}^{|L(u)|} = \{x_i - u\}_{i \in L(u)}. \quad (10)$$

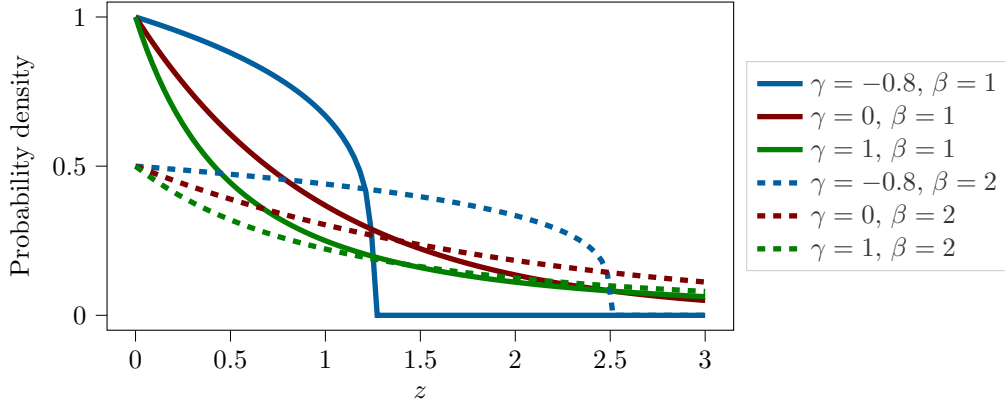


Figure 1: Probability density of the GPD, i.e., the derivative of Eq. (11), for different values of the shape parameter, γ , and the scale parameters β .

Here, $|L(u)|$ denotes the cardinality of $L(u)$, i.e., the number of parameter values of the set $\{x_i\}_{i=1}^N$ that are above the threshold u . Following (Franke et al., 2004), under a mild assumption¹ regarding the underlying distribution of x , the distribution of the excess value y approaches the GPD as $u \rightarrow \infty$. The GPD is given by:

$$G(z) = \begin{cases} 1 - \left(1 + \frac{\gamma z}{\beta}\right)^{-\frac{1}{\gamma}} & \text{if } \gamma \neq 0 \\ 1 - \exp\left\{-\frac{z}{\beta}\right\} & \text{if } \gamma = 0 \end{cases}, \quad (11)$$

where the support is $z \geq 0$ for $\gamma \geq 0$ and $0 \leq z \leq -\beta/\gamma$ for $\gamma < 0$. The two parameters of the GPD are the so-called shape parameter, γ , and the scale parameter, $\beta > 0$. Figure 1 shows the probability density of the GPD for different values of γ and β .

To determine the parameter range using the GPD, we simply assume that there is no lower bound or $x_L = -\infty$. The upper bound is found using the following equation:

$$\mathbb{E}[n_C] \cdot \mathbb{P}(x > u) \cdot (1 - G(x_U - u)) = \epsilon_F. \quad (12)$$

Here, the probability $\mathbb{P}(x > u)$ can simply be estimated by dividing the total number of parameter values that exceed u by the total number of scenarios in scenario category \mathcal{C} , i.e.,

$$\mathbb{P}(x > u) = \frac{|L(u)|}{N}. \quad (13)$$

To use Eq. (12), u must be chosen such that $\mathbb{E}[n_C] \cdot \mathbb{P}(x > u) \geq \epsilon_F$. In practice, this is not a problem because ϵ_F is generally small. Nevertheless, if it would result in a too low value of u , one can simply estimate the upper bound using $\mathbb{E}[n_C] \cdot \mathbb{P}(x > x_U) = \epsilon_F$.

The reason why we have assumed that $d = 1$ is that, in that case, it is straightforward to order the data. For example, it is straightforward to determine which scenario parameters are larger than the threshold

¹The distribution of x must be contained in the maximum domain of attraction of the generalized extreme value distribution. For more details, see (Balkema and De Haan, 1974; Pickands, 1975).

u. When considering multiple parameters per scenario ($d > 1$), one option is to only estimate an upper bound for one parameter and assume that all possible values for the remaining parameters are reasonably foreseeable. A second option is to assume independence of the different parameters. The approach presented in this section can easily be expanded to consider multiple independent parameters. A third option is to use a function for mapping the d -dimensional parameter space to a one-dimensional parameter space. In that case, the presented approach can be used to find an upper bound in the one-dimensional parameter space and this upper bound can be mapped to the d -dimensional parameter space using the inverse of the function that is used for the mapping.

2.2. Determining what reasonably preventable means

To answer Research question 2, this section proposes a method for quantifying the extent to which collisions are preventable. This is achieved by considering a skilled and attentive human driver as a benchmark for an ADS. Therefore, we will estimate the probability that a skilled and attentive human driver is able to prevent collisions. In Section 2.2.1, we first estimate to which extent a skilled and attentive human driver can avoid collisions considering all scenarios within a scenario category. We will employ Monte Carlo simulations using importance sampling to estimate this probability (de Gelder et al., 2021). As an alternative approach, in Section 2.2.2, we estimate to which extent a skilled and attentive human driver can avoid a collision considering a specific scenario.

2.2.1. Collision probability considering a scenario category

As already introduced in Section 2.1.3, it is assumed that the scenarios of a scenario category \mathcal{C} can be described using a d -dimensional parameter vector $x \in \mathbb{R}^d$. Let the (stochastic) outcome of a simulation of a scenario with parameters x be denoted by $R(x)$, where $R(x) = 1$ means that the simulation of the scenario with parameters x ends with a collision and otherwise $R(x) = 0$. To estimate the extent to which a skilled and attentive human driver can avoid collisions considering all scenarios of a scenario category, we estimate the expectation of $R(x)$, i.e., $\mathbb{E}[R(x)]$. The skilled and attentive human driver is modeled with a driver behavior model, see Section 3.3 for more details. To estimate this expectation, the PDF of x , denoted by $\hat{f}_{\mathcal{C}}(\cdot)$, needs to be estimated. For this, the KDE of Eq. (2) is used. With (crude) Monte Carlo sampling, $\mathbb{E}[R(x)]$ is estimated by sampling the parameters from the PDF and averaging the results of the simulation runs. Sampling from $\hat{f}_{\mathcal{C}}(\cdot)$ is straightforward. First, an integer $j \in \{1, \dots, N\}$ is chosen randomly with each integer having equal likelihood. Next, a random sample is drawn from a Gaussian with covariance $h^2 I_d$ and mean x_j , where I_d denotes the d -by- d identity matrix.

With crude Monte Carlo, the probability of a collision is calculated by taking the mean of $R(x)$ over a large number, N_{MC} , of different realizations of x :

$$\mathbb{E}[R(x)] \approx \mu_{\text{MC}} = \frac{1}{N_{\text{MC}}} \sum_{j=1}^{N_{\text{MC}}} R(x_j), \quad x_j \sim \hat{f}_{\mathcal{C}}. \quad (14)$$

It is easy to see that the crude Monte Carlo result is unbiased, i.e., $\mathbb{E}[\mu_{\text{MC}}] = \mathbb{E}[R(x)]$. To estimate the potential approximation error, $\mu_{\text{MC}} - \mathbb{E}[R(x)]$, the estimated standard deviation of Eq. (14) is commonly used:

$$\sigma_{\text{MC}} = \frac{1}{N_{\text{MC}}} \sqrt{\sum_{j=1}^{N_{\text{MC}}} (\mu_{\text{MC}} - R(x_j))^2}. \quad (15)$$

In general, it can be expected that the probability of collision, $\mathbb{E}[R(x)]$, is small. As a result, none or few of the N_{MC} scenario simulations may end with a collision and the relative uncertainty, i.e., $\sigma_{\text{MC}}/\mu_{\text{MC}}$, will be high or undefined (in case none of the scenario simulations ends with a collision). With importance sampling, the scenario parameters are sampled from a different distribution — the so-called importance density — such that the simulation runs focus more on scenarios in which the probability of collision is high. This will lead to a lower relative uncertainty of the estimated probability of collision. We use nonparametric importance sampling, which means that a nonparametric method is used to estimate the unknown optimal importance density (Zhang, 1996). More specifically, as proposed in (Zhang, 1996; de Gelder and Paardekooper, 2017), the nonparametric importance sampling method employs KDE to construct the importance density.

In particular, this work uses the importance density $g(\cdot)$, which is defined as follows:

$$g(x) = \frac{1}{N_C h_{\text{NIS}}^d} \sum_{i=1}^{N_C} K\left(\frac{1}{h_{\text{NIS}}} (x - x_{(i)})\right). \quad (16)$$

Here, $\{x_{(1)}, \dots, x_{(N_C)}\}$ denote the N_C “most critical” scenarios of the crude Monte Carlo sampling ($N_C < N_{\text{MC}}$). We use the N_C scenarios that resulted in the lowest minimum Time to Collision (TTC) (Hayward, 1972) during each simulation run to determine N_C “most critical” scenarios. The TTC is defined as the ratio of the distance toward an approaching object and the speed difference with that object. The bandwidth h_{NIS} is estimated using leave-one-out cross validation. If N_{NIS} scenarios are simulated in nonparametric importance sampling, the estimated probability of collision is

$$\mathbb{E}[R(x)] \approx \mu_{\text{NIS}} = \frac{1}{N_{\text{NIS}}} \sum_{j=1}^{N_{\text{NIS}}} R(x_j) \frac{\hat{f}_{\mathcal{C}}(x_j)}{g(x_j)}, \quad x_j \sim g. \quad (17)$$

The weight $\hat{f}_{\mathcal{C}}(x_j)/g(x_j)$ is used to correct for the bias introduced by sampling from $g(\cdot)$ instead of $\hat{f}_{\mathcal{C}}(\cdot)$. Because $g(x) > 0$ whenever $R(x)\hat{f}_{\mathcal{C}}(x) > 0$, Eq. (17) gives unbiased results (Owen, 2013). The estimated standard deviation of Eq. (17) is

$$\sigma_{\text{NIS}} = \frac{1}{N_{\text{NIS}}} \sqrt{\sum_{j=1}^{N_{\text{NIS}}} \left(\frac{R(x_j)\hat{f}_{\mathcal{C}}(x_j)}{g(x_j)} - \mu_{\text{NIS}} \right)^2}. \quad (18)$$

For more details regarding the nonparametric importance sampling, the reader is referred to (de Gelder et al., 2021).

2.2.2. Collision probability considering a scenario

To determine the probability of a collision considering a specific scenario with parameters x , we can simulate that specific scenario. As introduced in Section 2.2.1, the outcome of a simulation of a scenario with parameters x is denoted by $R(x)$, where $R(x) = 1$ indicates that the simulation ended with a collision and $R(x) = 0$ otherwise. Let $C(x)$ denote the probability that a skilled and attentive human driver does not prevent a collision. If the simulation is fully deterministic, a single simulation suffices. If this is not the case, a straightforward way to compute the collision probability is to repeat a certain number of simulations with the same x and count the number of simulations that result in a collision. If N_{sim} denotes the number of simulations, then the probability of a collision can be estimated using

$$C(x) = \frac{N_{\text{col}}(x)}{N_{\text{sim}}}, \quad (19)$$

where $N_{\text{col}}(x) = \sum_{j=1}^{N_{\text{sim}}} R(x)$ denotes the number of simulation runs that end in a collision.

To determine whether it is reasonable to assume that a human cannot avoid a collision, we are interested in the cases where $C(x) > C_p$, where C_p denotes a certain threshold. Therefore, the exact value of $C(x)$ is less relevant. This knowledge is used to limit the number of simulations that needs to be conducted for each scenario with parameters x . The number of simulations, N_{sim} , is increased until the certainty that $C(x)$ is below or above C_p is more than $1 - \alpha$, where α denotes the probability of a wrong conclusion regarding $C(x) > C_p$. This certainty is computed using the binomial distribution. In other words, N_{sim} is increased until one of the following conditions is reached:

$$\sum_{k=0}^{N_{\text{col}}(x)} \text{Bin}(k, C_p, N_{\text{sim}}) < \alpha, \quad (20)$$

$$\sum_{k=N_{\text{col}}(x)}^{N_{\text{sim}}} \text{Bin}(k, C_p, N_{\text{sim}}) < \alpha, \quad (21)$$

with

$$\text{Bin}(k, p, n) = \frac{n!}{k!(n-k)!} p^k (1-p)^{n-k}. \quad (22)$$

In practice, using Eqs. (20) and (21) with $C_p = 0.5$ and $\alpha = 0.01$, it means that a minimum of seven simulation runs are conducted. To limit the number of simulation runs, especially when $C(x) \approx C_p$, N_{sim} is further limited to 100.

3. Analysis and Results

To illustrate the proposed method for determining in a quantitative manner what are reasonably foreseeable scenarios and preventable collisions, the method is applied in a case study. This case study considers three scenario categories that are detailed in Section 3.1. Details regarding the used data set are mentioned in Section 3.2. In this case study, a model is used to describe the driver behavior, see Section 3.3. Finally,

Sections 3.4 and 3.5 present the results regarding the reasonably foreseeable scenarios and the preventable collisions, respectively.

3.1. Scenarios and parameterization

This case study considers three scenario categories. The first scenario category is named “Leading Vehicle Decelerating (LVD)” and denoted by \mathcal{C}_{LVD} . This is one of the two scenario categories that are mentioned as possibly “critical scenarios” in the ALKS regulation (E/ECE/TRANS/505/Rev.3/Add.156, 2021). The scenarios that belong to this scenario category consider a leading vehicle that is driving in front of the ego vehicle. Initially, this leading vehicle is driving at a constant speed $v_{1,0} > 0$. The leading vehicle decelerates such that its end speed is $v_{1,0} - \Delta_v$, with $0 < \Delta_v < v_{1,0}$. The average deceleration of the leading vehicle is denoted by $\bar{a} > 0$. To model the speed of the leading vehicle during its deceleration activity, a sinusoidal shape is assumed. It is further assumed that the ego vehicle is initially driving behind the leading vehicle at a constant distance and speed and that the desired speed of the ego vehicle equals the initial speed. The parameter vector that describes LVD scenarios contains the initial speed of the leading vehicle ($v_{1,0}$), the ratio of the speed difference and the initial speed ($\Delta_v/v_{1,0}$), and the average deceleration (\bar{a}):

$$x^\top = \begin{bmatrix} v_{1,0} & \Delta_v/v_{1,0} & \bar{a} \end{bmatrix}. \quad (23)$$

Note that because of the infinite support of the Gaussian kernel of Eq. (3), the kernel density estimator will assign a positive density for parameter values that are invalid. For the first parameter, this is insignificant, so the PDF is simply set to zero for $v_{1,0} \leq 0$. The resulting PDF is rescaled such that it still integrates to 1. For the other two parameters, however, we have mapped the parameter before applying the KDE, such that there is no positive density for parameter values that are invalid. First, instead of using $\Delta_v/v_{1,0}$, which is between 0 and 1, we use $-\log(v_{1,0}/\Delta_v - 1)$ and for \bar{a} , which is larger than 0, $\log \bar{a}$ is used. In the remainder of this work, although we use the mapped parameters for the density estimation, the results and figures show the parameters of Eq. (23) as these are easier to interpret than the mapped parameters.

The second scenario category is named “cut-in” and denoted by $\mathcal{C}_{\text{cut-in}}$. This scenario category is the other scenario category that is mentioned as a potentially “critical scenario” in the ALKS regulation (E/ECE/TRANS/505/Rev.3/Add.156, 2021). Cut-in scenarios consider a vehicle that suddenly cuts into the lane of the ego vehicle such that this vehicle becomes the leading vehicle of the ego vehicle. At the moment of the cut-in, the longitudinal gap between the two vehicles is $g_0 > 0$. For similar reasons as explained for the LVD scenario, for the KDE, $\log g_0$ is used instead of g_0 . It is assumed that the vehicle that performs the cut-in drives at a constant speed which is denoted by $v_1 > 0$. The initial speed of the ego vehicle is denoted by $v_{e,0} > 0$. The parameter vector that describes cut-in scenarios contains initial gap (g_0), the initial speed of the ego vehicle ($v_{e,0}$), and the ratio of the initial speeds of the leading vehicle and the ego vehicle ($v_1/v_{e,0}$):

$$x^\top = \begin{bmatrix} g_0 & v_{e,0} & v_1/v_{e,0} \end{bmatrix}. \quad (24)$$

The third scenario category is named “Approaching Slower Vehicle (ASV)” and denoted by \mathcal{C}_{ASV} . This scenario category ASV, which also includes scenarios in which the leading vehicle is stationary at standstill, accounts for more than 25 % of all crashes that involve two vehicles in the U.S.A. (Najm et al., 2007). In an ASV scenario, the ego vehicle is initially driving at a speed $v_{e,0} > 0$ while approaching a vehicle that is moving at constant speed of $0 \leq v_l < v_{e,0}$. The parameter vector that describes ASV scenarios contains the initial speed of the ego vehicle ($v_{e,0}$) and the ratio of the speeds of the leading vehicle and the ego vehicle ($v_l/v_{e,0}$):

$$x^T = \begin{bmatrix} v_{e,0} & v_l/v_{e,0} \end{bmatrix}. \quad (25)$$

3.2. Data set

To estimate the exposure and the PDFs of the scenario parameters, the data set described in (Paardekooper et al., 2019) is used. The data were recorded from a single vehicle in which 20 experienced drivers were asked to drive a prescribed route. Each driver drove the 50 km route six times, which resulted in 63 h of data. The route contains urban roads, rural roads, and highways. To measure the surrounding traffic, the vehicle was equipped with three radars and one camera. The surrounding traffic was measured by fusing the data of the radars and the camera as described in (Elfring et al., 2016).

To extract the scenarios from the data set, the approach described in (de Gelder et al., 2020a) is used. LVD scenarios are found by querying for a vehicle that has the tags “leading vehicle” and “decelerating” at the same time. Cut-in scenarios are found by querying for a vehicle that initially has the tags “changing lane” and “no leading vehicle” which changes into the tags “changing lane” and “leading vehicle” (de Gelder et al., 2020a). ASV scenarios are found by querying for a vehicle that has the tags “leading vehicle” and “driving slower”. In 63 hours of driving, 1300 LVD scenarios, 297 cut-in scenario, and 291 ASV scenarios have been found.

3.3. Modeling of the driver behavior

To model the driver behavior, the Intelligent Driver Model plus (IDM+) (Schakel et al., 2010) is used. The parameters of the IDM+ model are adopted from (Treiber et al., 2000) except for the desired time headway, which is set to 1.2 s (Schakel et al., 2010). The IDM+ is a so-called collision-free model, because collisions are always prevented, sometimes at the costs of a high deceleration and zero reaction time. To prevent the use of unrealistic reaction times, we assume that the driver has a reaction time that is distributed according to a log-normal distribution with a mean of 0.92 s and a standard deviation of 0.28 s (Green, 2000). In addition, the maximum braking capacity is set to 6 m/s². Furthermore, it is assumed that the driver does not respond to vehicles that are further than 150 m away.

3.4. Results for reasonably foreseeable scenarios

Figure 2 shows the results for the LVD scenarios using the approach outlined in Section 2.1.3. The data, which are shown by the histograms, are used to estimate the PDF using KDE. Because 1300 LVD scenarios

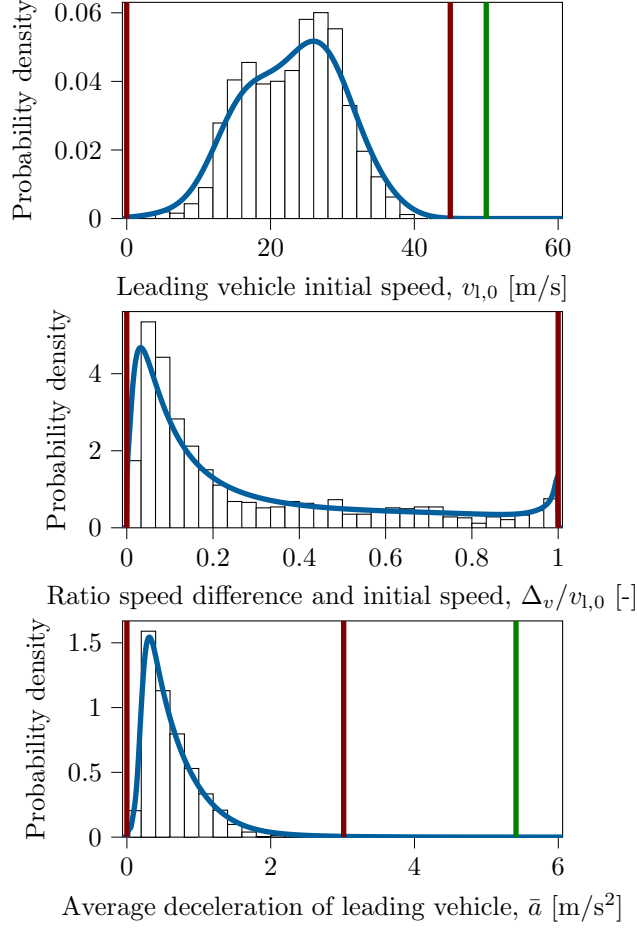


Figure 2: Result for reasonably foreseeable LVD scenarios using the approach of Section 2.1.3. The original data are represented by the histograms. The blue lines denote the estimated marginal distributions based on the KDE of Eq. (2). The red vertical lines show the boundaries of the reasonably foreseeable parameter range with $\epsilon_F = 0.1 \text{ h}^{-1}$ and the green vertical lines show these boundaries with $\epsilon_F = 0.01 \text{ h}^{-1}$ (if different).

have been observed in 63 hours of driving, it follows that $\mathbb{E}[n_{\mathcal{C}_{\text{LVD}}}] = 20.6 \text{ h}^{-1}$. Therefore, if $\epsilon_F = 0.1 \text{ h}^{-1}$, it follows from Eq. (8) that we look for the range $[x_L, x_U]$ such that $\mathbb{P}(x \in [x_L, x_U]) = 0.9951$. The red vertical lines in Figure 2 show one possibility for x_L and x_U such that $\mathbb{P}(x \in [x_L, x_U]) = 0.9951$. Here, $x_L^T = [0 \text{ m/s} \ 0 \ 0 \text{ m/s}^2]$ and $x_U^T = [45.0 \text{ m/s} \ 1 \ 3.01 \text{ m/s}^2]$. With $\epsilon_F = 0.01 \text{ h}^{-1}$, the same lower bound could be used with an upper bound $x_U^T = [50.0 \text{ m/s} \ 1 \ 5.41 \text{ m/s}^2]$, such that $\mathbb{P}(x \in [x_L, x_U]) = 0.9995$.

Figure 3 shows the result for LVD scenarios using the approach outlined in Section 2.1.4. We only look at the upper bound of the average deceleration. The threshold $u = 1.18 \text{ m/s}^2$ is chosen such that 10% of the data is used for the set of excess values, i.e., $\mathbb{P}(\bar{a} > u) = 0.1$. Figure 3 shows the histogram of these excess values. Fitting the parameters of the GPD of Eq. (11) on these excess values using the maximum likelihood method resulted in $\gamma = 0.051$ and $\beta = 0.36 \text{ m/s}^2$. Using Eq. (12) with $\epsilon_F = 0.1 \text{ h}^{-1}$ results in an upper bound of $\bar{a} = 2.34 \text{ m/s}^2$, see the red vertical line in Figure 3. In other words, based on this approach

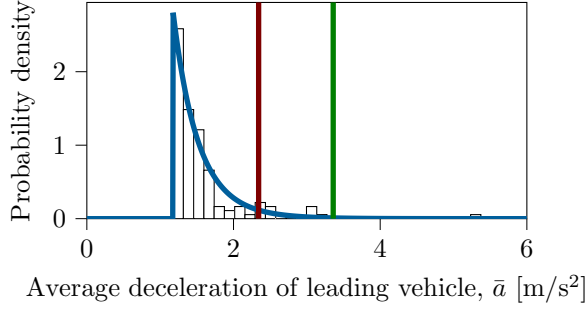


Figure 3: Result for reasonably foreseeable LVD scenarios using the approach of Section 2.1.4. The histogram represents 10 % of the data with the highest average deceleration. The blue line is the probability density of the fitted GPD of Eq. (11). The red (green) vertical line at $\bar{a} = 2.34 \text{ m/s}^2$ ($\bar{a} = 3.36 \text{ m/s}^2$) denotes the upper bound if $\epsilon_F = 0.1 \text{ h}^{-1}$ ($\epsilon_F = 0.01 \text{ h}^{-1}$) is used.

with the threshold $\epsilon_F = 0.1 \text{ h}^{-1}$, all LVD scenarios with $\bar{a} \leq 2.34 \text{ m/s}^2$ are reasonably foreseeable and all LVD scenarios with $\bar{a} > 2.34 \text{ m/s}^2$ are not reasonably foreseeable. With $\epsilon_F = 0.01 \text{ h}^{-1}$, the upper bound shifts to $\bar{a} = 3.36 \text{ m/s}^2$. Note that using this approach, the other scenario parameters, $v_{l,0}$ and $\Delta_v/v_{l,0}$, are not used to determine whether a scenario is reasonably foreseeable.

Figure 4 shows the results for the cut-in scenarios using the approach outlined in Section 2.1.3. In total, 297 cut-in scenarios have been observed, so $\mathbb{E}[n_{\text{cut-in}}] = 297/63 \text{ h} = 4.71 \text{ h}^{-1}$. So, with a threshold of $\epsilon_F = 0.1 \text{ h}^{-1}$, we look for the range $[x_L, x_U]$ such that $\mathbb{P}(x \in [x_L, x_U]) = 0.9788$. This probability is obtained using $x_L^T = [3.14 \text{ m} \quad 0 \text{ m/s} \quad 0.700]$ and $x_U^T = [120 \text{ m} \quad 50.0 \text{ m/s} \quad 2.00]$, see the red vertical lines in Figure 4. When using a threshold $\epsilon_F = 0.01 \text{ h}^{-1}$, the parameter range of reasonably foreseeable scenarios becomes substantially larger with $x_L^T = [0.900 \text{ m} \quad 0 \text{ m/s} \quad 0.100]$ and $x_U^T = [120 \text{ m} \quad 50.0 \text{ m/s} \quad 2.00]$.

Figure 5 shows the result for cut-in scenarios using the approach based on the EVT. We look at the ratio of the leading vehicle speed and the initial ego vehicle speed, $v_l/v_{e,0}$. If this ratio is below one, the ego vehicle needs to perform an evasive action, e.g., by braking or steering. Typically, for lower values of $v_l/v_{e,0}$, a stronger evasive maneuver is expected. Therefore, we are interested in the lower bound of $v_l/v_{e,0}$ rather than the upper bound. To use the approach as outlined in Section 2.1.4, we simply estimate the upper bound of $-v_l/v_{e,0}$. We use a threshold of $u = -0.91$ because 10 % of the values of $v_l/v_{e,0}$ are below 0.91. Figure 5 shows the histogram of these excess values. Note that the data and the upper bound of $-v_l/v_{e,0}$ are (again) multiplied with -1 , such that the x-axis represents $v_l/v_{e,0}$ and the upper bound represents the lower bound of $v_l/v_{e,0}$. Fitting the parameters of the GPD of Eq. (11) on these excess values using the maximum likelihood method resulted in $\gamma = 0.62$ and $\beta = 0.045$. Because we assume that $v_l/v_{e,0} > 0$, the fitted PDF is set to zero if $v_l/v_{e,0} \leq 0$ and the PDF is rescaled such that the PDF integrates to 1. Using Eq. (12) with $\epsilon_F = 0.1 \text{ h}^{-1}$ results in a lower bound of $v_l/v_{e,0} = 0.81$, see the red vertical line in Figure 3. With $\epsilon_F = 0.01 \text{ h}^{-1}$, the lower bound shifts to $v_l/v_{e,0} = 0.42$.

Figure 6 shows the results for the ASV scenarios using the approach outlined in Section 2.1.3. In total,

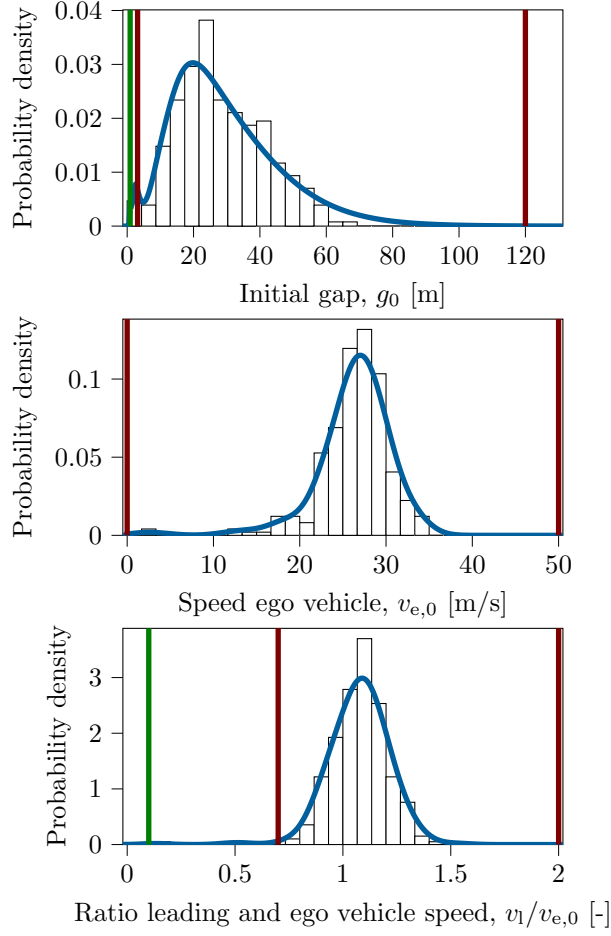


Figure 4: Result for reasonably foreseeable cut-in scenarios using the approach of Section 2.1.3. For a more detailed explanation, see Figure 2.

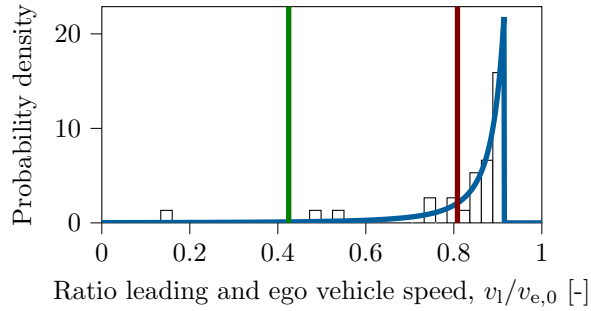


Figure 5: Result for reasonably foreseeable cut-in scenarios using the approach of Section 2.1.4. The histogram represents 10% of the data with the smallest ratio of leading vehicle speed and the initial ego vehicle speed, $v_l/v_{e,0}$. The blue line is the probability density of the fitted GPD of Eq. (11). The red (green) vertical line at $v_l/v_{e,0} = 0.81$ ($v_l/v_{e,0} = 0.42$) denotes the lower bound if $\epsilon_F = 0.1 \text{ h}^{-1}$ ($\epsilon_F = 0.01 \text{ h}^{-1}$) is used.

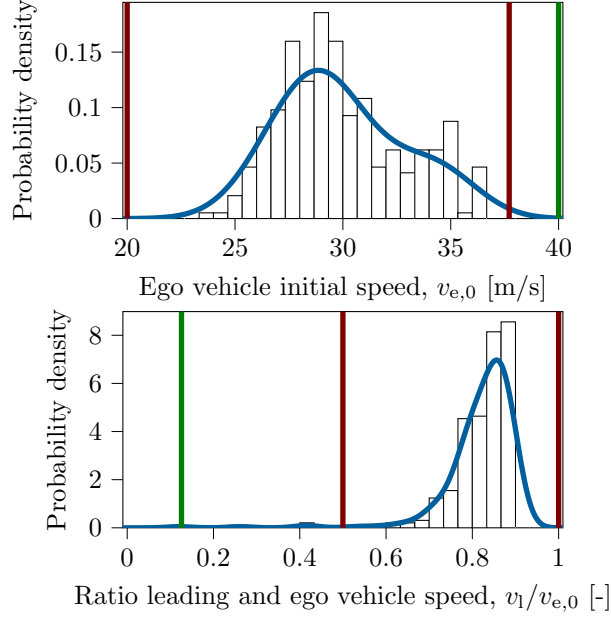


Figure 6: Result for reasonably foreseeable ASV scenarios using the approach of Section 2.1.3. For a more detailed explanation, see Figure 2.

291 ASV scenarios have been observed, so $\mathbb{E}[n_{C_{ASV}}] = 291/63 \text{ h} = 4.63 \text{ h}^{-1}$. One option for the range $[x_L, x_U]$ to satisfy Eq. (8) with $\epsilon_F = 0.1 \text{ h}^{-1}$ is $x_L^T = [20.0 \text{ m/s} \quad 0.50]$ and $x_U^T = [37.7 \text{ m/s} \quad 1.0]$, see the red vertical lines in Figure 6. With $\epsilon_F = 0.01 \text{ h}^{-1}$, the upper bound of the initial ego vehicle speed, $v_{e,0}$, shifts to 40 m/s and the lower bound of the ratio of leading vehicle speed and the initial ego vehicle speed, $v_l/v_{e,0}$, shifts to 0.13, see the green vertical lines in Figure 6.

For the approach using the EVT, the same steps as for the cut-in scenarios are followed, see Figure 7. This results in a lower bound of $v_l/v_{e,0} = 0.62$ with $\epsilon_F = 0.1 \text{ h}^{-1}$ and a lower bound of $v_l/v_{e,0} = 0.27$ with $\epsilon_F = 0.01 \text{ h}^{-1}$.

3.5. Results for preventable collisions

First, the probability that a human driver cannot avoid a collision in scenarios that belong to a specific scenario category is estimated using the approach outlined in Section 2.2.1. As explained in Section 2.2.1, Monte Carlo simulations have been conducted. Using the estimated PDF of the scenario parameters (see Figures 2, 4 and 6) for sampling, $N_{MC} = 10000$ simulations have been conducted. The results of these simulations are reported in Table 2. From the 10000 LVD scenarios, 9 scenarios resulted in a collision and 24 of the 10000 simulations of the cut-in scenarios has resulted in a collision. None of the 10000 ASV scenarios resulted in a collision. This illustrates the need for a more efficient sampling strategy, as also explained in Section 2.2.1. When applying importance sampling, the estimated probability of a collision in an LVD scenario is $7.81 \cdot 10^{-4}$ with an estimated uncertainty of $5.51 \cdot 10^{-5}$. Similarly, the estimated

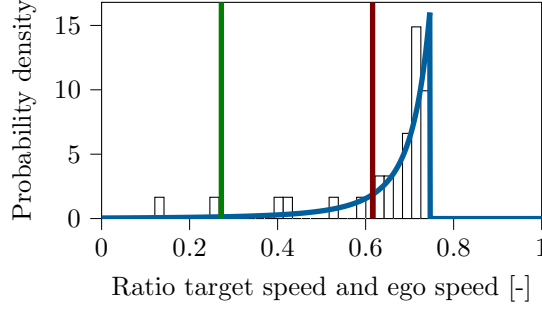


Figure 7: Result for reasonably foreseeable ASV scenarios using the approach of Section 2.1.4. The histogram represents 10 % of the data with the smallest ratio of leading vehicle speed and the initial ego vehicle speed, $v_l/v_{e,0}$. The blue line is the probability density of the fitted GPD of Eq. (11). The red (green) vertical line at $v_l/v_{e,0} = 0.62$ ($v_l/v_{e,0} = 0.27$) denotes the lower bound if $\epsilon_F = 0.1 \text{ h}^{-1}$ ($\epsilon_F = 0.01 \text{ h}^{-1}$) is used.

Table 2: Probability that a human driver cannot avoid a collision.

Scenario category	μ_{MC} of Eq. (14)	σ_{MC} of Eq. (15)	μ_{NIS} of Eq. (17)	σ_{NIS} of Eq. (18)
\mathcal{C}_{LVD}	$9.00 \cdot 10^{-4}$	$3.00 \cdot 10^{-3}$	$7.81 \cdot 10^{-4}$	$5.51 \cdot 10^{-5}$
\mathcal{C}_{cut-in}	$2.40 \cdot 10^{-3}$	$4.89 \cdot 10^{-4}$	$2.06 \cdot 10^{-3}$	$6.53 \cdot 10^{-5}$
\mathcal{C}_{ASV}	0.0	0.0	$2.56 \cdot 10^{-6}$	$2.05 \cdot 10^{-6}$

probabilities of a collision in cut-in and ASV scenarios are $2.06 \cdot 10^{-3}$ and $2.56 \cdot 10^{-6}$, respectively.

Figure 8 shows the result of reasonably preventable collisions in LVD scenarios. We have used the approach described in Section 2.2.2 with $C_p = 0.5$ and $\alpha = 0.01$. The parameters x for which the probability that a skilled and attentive human collides, i.e., $C(x)$, is estimated are taken from a grid with:

- 100 values of $\Delta_v/v_{l,0}$ ranging from zero to one;
- 100 values of \bar{a} ranging from 3.5 m/s^2 to 5.41 m/s^2 , where this latter value is the upper bound determined using the estimated PDF with $\epsilon_F = 0.01 \text{ h}^{-1}$ (see Figure 2); and
- $v_{l,0}$ ranging from 10 m/s to 50 m/s in steps of 10 m/s , where 50 m/s is the upper bound determined using the estimated PDF with $\epsilon_F = 0.01 \text{ h}^{-1}$ (see Figure 2).

Each line in Figure 8 shows where $C(x) \approx 0.5$ for a specific value of $v_{l,0}$. In each case, the parameter region below the line is where the collision probability is below 0.5 while the region above the line is where the collision probability is above 0.5. For example, if $\Delta_v/v_{l,0} = 0.85$ and $\bar{a} = 5 \text{ m/s}^2$, a collision is reasonably preventable in case $v_{l,0} = 10 \text{ m/s}$ or $v_{l,0} = 20 \text{ m/s}$ while a collision is not reasonably preventable with these values of $\Delta_v/v_{l,0}$ and \bar{a} if $v_{l,0} = 30 \text{ m/s}$, $v_{l,0} = 40 \text{ m/s}$, or $v_{l,0} = 50 \text{ m/s}$.

Figure 9 presents the result of reasonably preventable collision in cut-in scenarios, which are obtained in a similar way as the results of the LVD scenarios in Figure 8. Figure 9 shows that if $v_{e,0} = 50 \text{ m/s}$, there is a large range for g_0 and $v_l/v_{e,0}$ for which a collision is not reasonably preventable, i.e., the region on the left

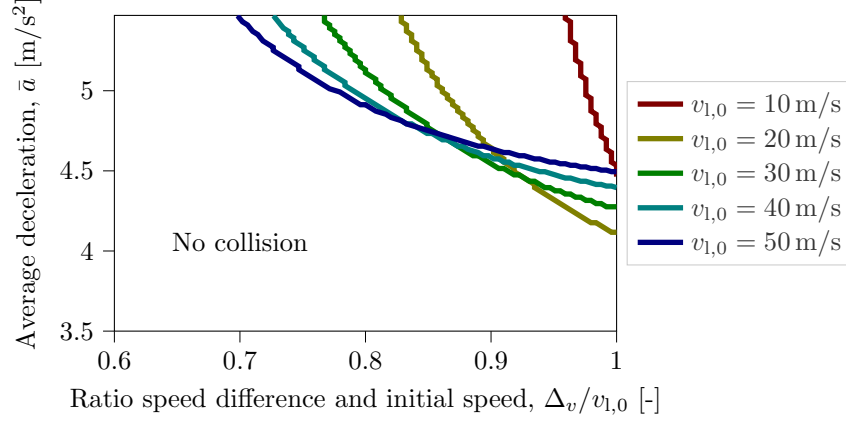


Figure 8: Lines that split the parameter space of the LVD scenarios into a region where the estimated probability that a skilled and attentive human collides is smaller than $C_p = 0.5$ (i.e., $C(x) < C_p$) (lower left region) and larger than $C_p = 0.5$ (i.e., $C(x) > C_p$) (upper right region).

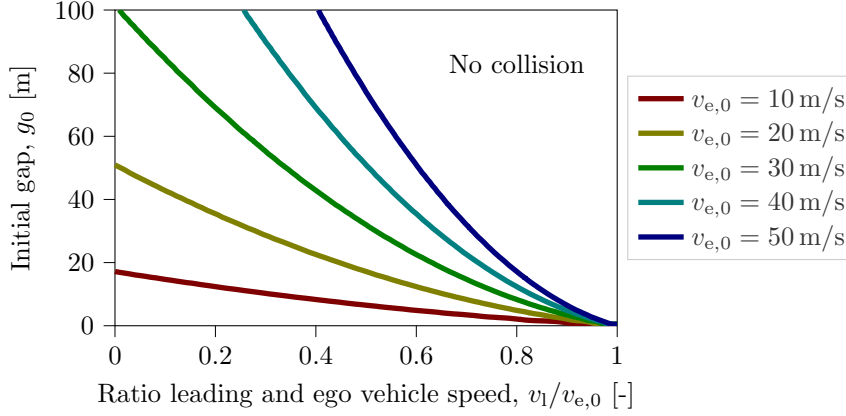


Figure 9: Lines that split the parameter space of the cut-in scenarios into a region where $C(x) < C_p$ (upper right region) and $C(x) > C_p$ (lower left region) with $C_p = 0.5$.

of the blue line. For smaller values of $v_{e,0}$, this region becomes smaller. For example, if $v_{e,0} = 10$ m/s, all cut-in scenarios with $g_0 > 20$ m are reasonably preventable, i.e., the region above the red line in Figure 9.

We have also conducted simulations of the ASV scenarios. Based on the parameter range determined using the estimated PDF with $\epsilon_F = 0.01 \text{ h}^{-1}$ (see Figure 6), simulations has been conducted with $v_{e,0}$ ranging from 20 m/s to 40 m/s and $v_l/v_{e,0}$ ranging from 0.13 to one. In all cases, the estimated probability that a skilled and attentive human driver does not prevent a collision is below $C_p = 0.5$.

4. Discussion

This paper presented a method to determine which scenarios are reasonably foreseeable and to which extent collisions are preventable. Given the approved United Nations regulation that states that “the activated system shall not cause any collisions that are reasonably foreseeable and preventable” (E/ECE/TRANS/505/Rev.3/Add.156

2021, Clause 5.1.1), the results of the presented method can be used to identify in which scenarios an ADS is expected to avoid collisions. This section discusses the approaches and results that are presented and some directions for future research. The discussion in Section 4.1 is related to Research question 1 and the discussion in Section 4.2 is related to Research question 2.

4.1. Discussion related to reasonably foreseeable scenarios

Two different approaches to determine what are reasonably foreseeable scenarios have been presented. Both approaches estimate a range for the parameters that describe the scenarios that belong to a specific scenario category. The first approach (Section 2.1.3) estimates a PDF of the parameters using KDE. An advantage of this approach is that no strong assumptions regarding the shape of the PDF are considered. However, near the tails of the estimated PDF, the influence of the choice of the kernel becomes more apparent. The Gaussian kernel of Eq. (3) is opted because it makes evaluating the CDF feasible. Choosing a kernel from the family of multivariate beta kernels (Duong, 2015), such as the multivariate uniform or Epanechnikov kernel, would require numerical integration. This becomes very cumbersome, especially because a high numerical precision is required for low values of ϵ_F . Apart from the practical advantage, there is no argument that justifies the choice of the Gaussian kernel. Hence, if the estimated bounds are beyond the most extreme data points that are used to construct the kernel density estimator, then the precision of these bounds may be low. In our case study, this is the case when $\epsilon_F = 0.01 \text{ h}^{-1}$ is used.

The alternative approach is based on the EVT (Section 2.1.4) and uses a fitted GPD to determine the upper bound of a scenario parameter. The advantage of this approach is that the EVT justifies the choice of the GPD. EVT has successfully been used to determine extremes that are beyond the most extreme values in the data (de Haan, 1994; Tarko, 2012). A disadvantage of this approach is that it is typically applied to only one parameter, although it is possible to extend it to multiple parameters, e.g., using a mapping of multiple parameters to one parameter.

Similar as in (Nakamura et al., 2022; Muslim et al., 2023), both approaches presented in this work construct a PDF which is used to estimate the range of the parameters of the reasonably foreseeable scenarios. Our proposed methods differ from the method used in (Nakamura et al., 2022; Muslim et al., 2023) because fewer assumptions regarding the PDF estimation are made. In (Nakamura et al., 2022; Muslim et al., 2023), it is assumed that the scenario parameters are independent, that the parameters are distributed according to the Beta distribution, and the lower and upper bounds of these Beta distributions are set to some assumed values. If we would use the method proposed in (Nakamura et al., 2022; Muslim et al., 2023), we would have reported a different outcome. We cannot objectively state which outcome is better because there is no objective truth. In general, however, we can state that if the assumptions made in (Nakamura et al., 2022; Muslim et al., 2023) are correct, it is likely that the outcome based on their method would be more accurate. On the other hand, if there is no reason to make certain assumptions regarding the PDF, it generally leads

to more accurate results if one does not rely on those assumptions. For our case study, we cannot justify the assumptions made in (Nakamura et al., 2022; Muslim et al., 2023). Thus, for our case study, the methods proposed in this work might be more suitable.

The proposed method for determining the reasonably foreseeable scenarios relies on data. It is, therefore, important that the data are adequate. This means that the data need to match the ODD of the ADS. For example, the data that have been used in the case study were obtained from driving a specific route multiple times during daytime and good weather conditions. If the ODD of the ADS considers the same route during daytime and good weather conditions, then the data are representing this ODD. If, however, the ODD is substantially different, extra arguments are needed to justify that the data still represent the ODD. The estimated exposure of the scenarios and the estimated parameter PDFs might not be accurate for the specified ODD in case the data have been recorded under different circumstances. As a result, the estimated parameter range of the reasonably foreseeable scenarios might not be accurate enough. The adequacy of the data also concerns the amount of data. It is important that we have enough data to accurately determine the PDF of the scenario parameters. As an order of magnitude, the number of hours of data must be roughly $1/\epsilon_F$.

An important parameter for determining the parameter range of the reasonably foreseeable parameters is ϵ_F . For the sake of illustration, in the case study, we have used $\epsilon_F = 0.1 \text{ h}^{-1}$ and $\epsilon_F = 0.01 \text{ h}^{-1}$, which means that, on average, one scenario in 10 or 100 hours of driving, respectively, is found with its parameters not within the range $[x_L, x_U]$. When deploying an ADS on a large scale, however, a much lower value of ϵ_F might be better. This automatically results in a larger parameter range of the reasonably foreseeable scenarios. The reason that the presented case study has used $\epsilon_F = 0.01 \text{ h}^{-1}$ as a minimum value is that the estimation of the reasonably foreseeable parameter range with 63 hours of data would be inaccurate. Smaller values of ϵ_F require more data to accurately determine the parameter range of the reasonably foreseeable scenarios.

Our work provides methods to determine the range of the parameter values of reasonably foreseeable scenarios for a given scenario category. As mentioned in Section 2.1.1, it might require many scenario categories to cover a given ODD. It remains future work to define a method that identifies all reasonably foreseeable scenarios, i.e., across all relevant scenario categories. The work of Kusano et al. (2022) already provides substantial work in this direction, as they have identified a large set of scenarios based on the combinations of so-called core scenarios and salient factors which are properties of the actors or scenes that may impact the performance of the system.

4.2. Discussion related to reasonably preventable collisions

In Section 2.2, two approaches are presented for studying the extent to which a collision is preventable. The first approach considers all scenarios that belong to a specific scenario category. A method is provided

to calculate the probability that a skilled and attentive human driver cannot avoid a collision. The result is a probability for a given scenario category that can be used by an Automated Vehicle (AV) developer as a benchmark. If an AV reports a lower probability of colliding in scenarios for all relevant scenario categories, then the AV may be considered safer than a skilled and attentive human driver. Note that it is still possible that the AV fails to avoid a collision in scenarios that a skilled and attentive human driver can handle safely: the collision probabilities consider all scenarios in a scenario category, so as long as the AV handles some scenarios in a scenario category better than a skilled and attentive human driver, the AV may handle other scenarios from the same scenario category worse without having a higher collision probability. It remains an open question whether this is acceptable to authorities and the general public.

The second approach for studying the extent to which a collision is preventable considers individual scenarios. Using this approach, it is expected that an AV can safely deal with each scenario that a skilled and attentive human driver can safely handle too. This might be closer to the intuition that an AV must prevent all collisions if it is reasonable to assume that a human driver can also prevent these collisions. A potential disadvantage of this approach, compared to the first approach, is that it might take a long time to study, design, and validate an AV that prevents all collisions that a skilled and attentive human driver can reasonably prevent. This might delay the actual deployment of AVs while the earlier introduction of AVs — that are potentially less safe — might actually have a positive impact on the overall traffic safety.

Note that both approaches can complement each other and that a combination is also possible, as already proposed by Kusano et al. (2022). The acceptance criterion for an ADS can be based on a comparison between the ADS and that (a model of) a skilled and attentive human driver — similar to the second approach — and, in addition, it can be required that the performance across all scenarios of a scenario category is at least comparable to a threshold — similar to the first approach.

The estimated probability that collisions are preventable by a skilled and attentive human driver strongly depends on the chosen human driver model. As a proof of concept, the case study has used a simple well-known driver behavior model with few adaptations. On the one hand, using a simple model contributes to the explainability of the results, ensures short simulation run times, and facilitates the reproducibility of the case study. On the other hand, the fidelity of the simulation results may be compromised by the simplicity of the human driver behavior model. When using the proposed method to assess the risk of deploying an ADS in the real world, evidence is needed to justify the fidelity of the simulation results. More research is needed to actually verify the fidelity of the simulation results.

Whereas the case study has employed a human driver behavior model, it is also possible to perform simulations with a real human, i.e., with driver-in-the-loop simulations. Given the number of simulation runs that has been conducted, it is impracticable to conduct all simulations with real humans, but a combination of driver-in-the-loop simulations and simulations with driver behavior models is possible. For example, the driver behavior models may be tuned to match the results of the driver-in-the-loop simulations such that

the simulations with the driver behavior models can be further used to interpolate the driver-in-the-loop simulation results.

In addition to driver-in-the-loop simulations, the results of the extent to which collisions are reasonably preventable could be compared to accident data. However, to truly compare the results of accident data with the results of the simulations of the skilled and attentive driver, only the accident data in which a skilled and attentive driver collided should be considered. Given a real-world accident, it might be challenging to determine, in hindsight, whether the drivers involved in the accident were skilled and attentive. The drivers' skills may be based on whether the drivers were (non-)professionals with certain number of years of experience, whether the drivers were involved in accidents before, etc. Especially the attentiveness might be challenging to determine in hindsight, especially if the accidents were fatal. Therefore, more research is needed to determine how and to which extent accident data can be used as a comparison of (driver-in-the-loop) simulations of skilled and attentive drivers.

5. Conclusions

The proposal for a new United Nations regulation concerning the approval of an Automated Driving System (ADS) has been an important milestone toward the deployment of highly-automated vehicles. This proposal has stated that “the activated system shall not cause any collisions that are reasonably foreseeable and preventable.” In this work, we have proposed novel methods to provide more clarity on the meaning of “reasonably foreseeable and preventable”. More specifically, the proposed methods provide two data-driven approaches to determine the scenarios that are “reasonably foreseeable” and, therefore, are to be considered during the development of an ADS. Furthermore, the proposed methods include two approaches to determine to which extent a skilled and attentive human driver is able to avoid collisions, i.e., to quantify whether or not in potentially critical scenarios, a collision is “reasonably preventable”. The result can be used as a benchmark for an ADS.

By means of a case study, the proposed methods have been illustrated. The case study has considered three types of scenarios: scenarios with a leading vehicle decelerating, cut-in scenarios, and scenarios in which the ego vehicle approaches a slower leading vehicle. For each of these three scenario categories, we have determined the ranges of the parameter values for the reasonably foreseeable scenarios. Furthermore, the likelihood that a skilled and attentive human driver cannot avoid a collision has been estimated using simulations.

Future work involves applying the proposed method with more data, thereby providing more accurate results. Additionally, it would be of interest to investigate appropriate values for the threshold that is used to determine the set of reasonably foreseeable scenarios. Other future work involves investigating whether the chosen human driver behavior model is appropriate and, if needed, improving the human driver behavior models to better mimic the behavior of a skilled and attentive human driver.

Acknowledgment

The work presented in this paper is part of the HEADSTART project. This project has received funding from the European Union’s Horizon 2020 research and innovation programme under grant agreement No. 824309. Content reflects only the authors’ view and European Commission is not responsible for any use that may be made of the information it contains.

References

- Aurora. The new era of mobility. Technical report, Aurora, 2019. URL https://downloads.ctfassets.net/v3j0gnq3qxwi/4QVMTwpBo2Z0mE03B09UP2/611de2c139aef05d7204ace06e946e00/VSSA_Final.pdf.
- A. A. Balkema and L. De Haan. Residual life time at great age. *The Annals of Probability*, 2(5):792–804, 1974. doi: 10.1214/aop/1176996548.
- K. Bimbraw. Autonomous cars: Past, present and future a review of the developments in the last century, the present scenario and the expected future of autonomous vehicle technology. In *12th International Conference on Informatics in Control, Automation and Robotics (ICINCO)*, volume 1, pages 191–198, 7 2015. URL <https://ieeexplore.ieee.org/abstract/document/7350466>.
- C.-Y. Chan. Advancements, prospects, and impacts of automated driving systems. *International Journal of Transportation Science and Technology*, 6(3):208–216, 2017. doi: 10.1016/j.ijtst.2017.07.008.
- E. de Gelder and J.-P. Paardekooper. Assessment of automated driving systems using real-life scenarios. In *IEEE Intelligent Vehicles Symposium (IV)*, pages 589–594, 2017. doi: 10.1109/ivs.2017.7995782.
- E. de Gelder, J. Manders, C. Grappiolo, J.-P. Paardekooper, O. Op den Camp, and B. De Schutter. Real-world scenario mining for the assessment of automated vehicles. In *IEEE International Transportation Systems Conference (ITSC)*, pages 1073–1080, 2020a. doi: 10.1109/ITSC45102.2020.9294652.
- E. de Gelder, O. Op den Camp, and N. de Boer. Scenario categories for the assessment of automated vehicles. Technical report, CETRAN, 2020b. URL http://cetransg/wp-content/uploads/2020/01/REP200121_Scenario_Categories_v1.7.pdf. Version 1.7.
- E. de Gelder, H. Elrofai, A. Khabbaz Saberi, O. Op den Camp, J.-P. Paardekooper, and B. De Schutter. Risk quantification for automated driving systems in real-world driving scenarios. *IEEE Access*, 9:168953–168970, 2021. doi: 10.1109/ACCESS.2021.3136585.
- E. de Gelder, J.-P. Paardekooper, A. Khabbaz Saberi, H. Elrofai, O. Op den Camp, S. Kraines, J. Ploeg, and B. De Schutter. Towards an ontology for scenario definition for the assessment of automated vehicles: An object-oriented framework. *IEEE Transactions on Intelligent Vehicles*, 7(2):300–314, 2022. doi: 10.1109/TIV.2022.3144803.
- L. de Haan. Extreme value statistics. In *Extreme Value Theory and Applications*, pages 93–122. Springer, 1994.
- T. Duong. ks: Kernel density estimation and kernel discriminant analysis for multivariate data in R. *Journal of Statistical Software*, 21(7):1–16, 2007. doi: 10.18637/jss.v021.i07.
- T. Duong. Spherically symmetric multivariate beta family kernels. *Statistics & Probability Letters*, 104:141–145, 2015. doi: 10.1016/j.spl.2015.05.012.
- ECE/TRANS/WP.29/2022/59/Rev.1. Proposal for the 01 series of amendments to un regulation no. 157 (automated lane keeping systems). Standard, World Forum for Harmonization of Vehicle Regulations, 2022. URL <https://unece.org/sites/default/files/2022-05/ECE-TRANS-WP.29-2022-59r1e.pdf>.
- E/ECE/TRANS/505/Rev.3/Add.156. Uniform provisions concerning the approval of vehicles with regard to automated lane keeping systems. Standard, World Forum for Harmonization of Vehicle Regulations, 2021. URL <https://unece.org/sites/default/files/2021-03/R157e.pdf>.
- J. Elfving, R. Appeldoorn, S. van den Dries, and M. Kwakernaat. Effective world modeling: Multisensor data fusion methodology for automated driving. *Sensors*, 16(10):1–27, 2016. doi: 10.3390/s16101668.
- J. Franke, W. K. Härdle, and C. M. Hafner. *Statistics of Financial Markets*, volume 2. Springer, 2004. doi: 10.1007/978-3-030-13751-9.
- General Motors. Self-driving safety report. Technical report, General Motors, 2018. URL <https://www.gm.com/content/dam/company/docs/us/en/gmcom/gmsafetyreport.pdf>.
- M. Green. “How long does it take to stop?” Methodological analysis of driver perception-brake times. *Transportation Human Factors*, 2(3):195–216, 2000. doi: 10.1207/sthf0203_1.
- J. C. Hayward. Near miss determination through use of a scale of danger. Technical Report TTSC-7115, Pennsylvania State University, 1972. URL <https://onlinepubs.trb.org/Onlinepubs/hrr/1972/384/384-004.pdf>.
- K. D. Kusano, K. Beatty, S. Schnelle, F. Favaro, C. Crary, and T. Victor. Collision avoidance testing of the waymo automated driving system. *arXiv preprint arXiv:2212.08148*, 2022. URL <https://arxiv.org/abs/2212.08148>.
- A. M. Madni. Autonomous system-of-systems. In *Transdisciplinary Systems Engineering*, pages 161–186. Springer, 2018. doi: 10.1007/978-3-319-62184-5_10.
- I. Mahdinia, R. Arvin, A. J. Khatkhat, and A. Ghiasi. Safety, energy, and emissions impacts of adaptive cruise control and co-operative adaptive cruise control. *Transportation Research Record*, 2674(6):253–267, 2020. doi: 10.1177/0361198120918572.

- A. Mammeri, G. Lu, and A. Boukerche. Design of lane keeping assist system for autonomous vehicles. In *7th International Conference on New Technologies, Mobility and Security (NTMS)*, pages 1–5, 2015. doi: 10.1109/NTMS.2015.7266483.
- K. Mattas, G. Albano, R. Donà, M. C. Galassi, R. Suarez-Bertoa, S. Vass, and B. Ciuffo. Driver models for the definition of safety requirements of automated vehicles in international regulations. application to motorway driving conditions. *Accident Analysis & Prevention*, 174:106743, 2022. doi: 10.1016/j.aap.2022.106743.
- D. Milakis, M. Snelder, B. van Arem, B. van Wee, and G. H. de Almeida Correia. Scenarios about development and implications of automated vehicles in the Netherlands. In *95th Annual Meeting Transportation Research Board*, 2016. URL https://www.researchgate.net/profile/Dimitris-Milakis/publication/288828248_Scenarios_about_development_and_implications_of
- H. Muslim, S. Endo, H. Imanaga, S. Kitajima, N. Uchida, E. Kitahara, K. Ozawa, H. Sato, and H. Nakamura. Cut-out scenario generation with reasonability foreseeable parameter range from real highway dataset for autonomous vehicle assessment. *IEEE Access*, 11:45349–45363, 2023. doi: 10.1109/ACCESS.2023.3268703.
- W. G. Najm, J. D. Smith, and M. Yanagisawa. Pre-crash scenario typology for crash avoidance research. Technical Report DOT HS 810 767, U.S. Department of Transportation Research and Innovative Technology Administration, 4 2007. URL https://rosap.ntl.bts.gov/view/dot/6281/dot_6281_DS1.pdf.
- H. Nakamura, H. Muslim, R. Kato, S. Préfontaine-Watanabe, H. Nakamura, H. Kaneko, H. Imanaga, J. Antona-Makoshi, S. Kitajima, N. Uchida, E. Kitahara, K. Ozawa, and S. Taniguchi. Defining reasonably foreseeable parameter ranges using real-world traffic data for scenario-based safety assessment of automated vehicles. *IEEE Access*, 10:37743–37760, 2022. doi: 10.1109/ACCESS.2022.3162601.
- A. B. Owen. Monte Carlo theory, methods and examples, 2013. URL <https://statweb.stanford.edu/~owen/mc/>.
- J.-P. Paardekooper, S. Montfort, J. Manders, J. Goos, E. de Gelder, O. Op den Camp, A. Bracquemond, and G. Thiolon. Automatic identification of critical scenarios in a public dataset of 6000 km of public-road driving. In *26th International Technical Conference on the Enhanced Safety of Vehicles (ESV)*, 2019. URL <https://www-esv.nhtsa.dot.gov/Proceedings/26/26ESV-000255.pdf>.
- E. Parzen. On estimation of a probability density function and mode. *The Annals of Mathematical Statistics*, 33(3):1065–1076, 1962. doi: 10.1214/aoms/1177704472.
- J. Pickands. Statistical inference using extreme order statistics. *The Annals of Statistics*, pages 119–131, 1975. doi: 10.1214/aos/1176343003.
- M. Rosenblatt. Remarks on some nonparametric estimates of a density function. *The Annals of Mathematical Statistics*, 27(3):832–837, 1956. doi: 10.1214/aoms/1177728190.
- SAE J3016. Taxonomy and definitions for terms related to driving automation systems for on-road motor vehicles. Technical report, SAE International, 4 2021.
- W. J. Schakel, B. van Arem, and B. D. Netten. Effects of cooperative adaptive cruise control on traffic flow stability. In *13th International IEEE Conference on Intelligent Transportation Systems*, pages 759–764, 2010. doi: 10.1109/itsc.2010.5625133.
- H.-P. Schoener. Challenging highway scenarios beyond collision avoidance for autonomous vehicle certification. *Researchgate preprint*, 2020. doi: 10.13140/RG.2.2.29355.05926.
- B. W. Silverman. *Density Estimation for Statistics and Data Analysis*. CRC press, 1986.
- A. P. Tarko. Use of crash surrogates and exceedance statistics to estimate road safety. *Accident Analysis & Prevention*, 45:230–240, 2012. doi: 10.1016/j.aap.2011.07.008.
- M. Treiber, A. Hennecke, and D. Helbing. Congested traffic states in empirical observations and microscopic simulations. *Physical review E*, 62(2):1805–1824, 2000. doi: 10.1103/PhysRevE.62.1805.
- B. A. Turlach. Bandwidth selection in kernel density estimation: A review. Technical report, Institut für Statistik und Ökonometrie, Humboldt-Universität zu Berlin, 1993. URL https://www.researchgate.net/publication/2316108_Bandwidth_Selection_in_Kernel_Density_Estimation_A_Review.
- N. E. Vellinga. Automated driving and the future of traffic law. In *Regulating New Technologies in Uncertain Times*, pages 67–82. Springer, 2019. doi: 10.1007/978-94-6265-279-8_5.
- Waymo. Waymo safety report. Technical report, Waymo, 2021. URL <https://downloads.ctfassets.net/sv23gofxcuiz/4gZ7ZUxd4SRj1D1W6z3rpf>
- P. Zhang. Nonparametric importance sampling. *Journal of the American Statistical Association*, 91(435):1245–1253, 1996. doi: 10.1080/01621459.1996.10476994.